Process Optimization Study of Etoricoxib Spray Dried Amorphous Solid Dispersion Containing HPMCAS

J. Tran-Dinh, M. Pimparade, M. Rane and A. Rajabi-Siahboomi
Colorcon, Inc. Harleysville, PA 19438, USA
www.colorcon.com

CRS
Poster Reprint 2019

Introduction

Hypromellose acetate succinate (HPMCAS) is a widely used polymer for improving the solubility of BCS Class II drugs by means of amorphous solid dispersions (ASD). HPMCAS is amenable to processing via hot melt extrusion (HME) or solvent based spray drying (SD) applications. Spray drying is a method that creates dry particles from a solvent based solution that is atomized through a nozzle and dried instantly, forming an amorphous solid dispersion of the drug in the polymer matrix. Process parameters that may be adjusted when spray drying can influence the final product. The purpose of this work was to evaluate critical process conditions for spray drying on ASDs of etoricoxib (ETO) and HPMCAS: solids content, spray nozzle diameter size and spray nozzle gas flow.

Methods

Nine solutions of 1:3 ratio ETO and HPMCAS (AFFINISOL™ 912G; International Flavors and Fragrances Inc.) in acetone were prepared and spray dried in a lab scale ProCept 4M8-TriX spray dryer at a spray rate of 5 g/min, air flow of 0.4 m3 /min and inlet air temperature of 80°C. Solids content, spray nozzle diameter and spray nozzle gas flow for all formulations were varied at low, medium and high levels (Table 1). The resulting ASDs were characterized by x-ray powder diffraction (XRPD; Equinox 100, Thermo Scientific, USA) and differential scanning calorimetry (DSC; Q200, TA Instruments, USA). Scanning electron microscopy (SEM; Phenom XL, Phenom World, USA) was used to investigate the morphology of ASDs. Particle size distributions of the powder samples were determined via laser diffraction (Mastersizer 2000, Malvern Instruments Ltd., UK). Thermal analysis of the powders was conducted via modulated DSC at a heating rate of 10°C/min., modulating ±2°C every 40 seconds. All the powder samples were tested for bulk density and true density. Dissolution testing was conducted using the ASDs containing 100 mg of drug in 1000 mL of phosphate buffer pH 6.8 using USP apparatus 2 (paddle) at 75 rpm. The samples were analyzed spectrophotometrically at 236 nm. Fusion Pro Software (S-Matrix Corporation) was used for analysis.

Table 1. Spray Drying Critical Process Parameters for ASD

Batch Name ASD	Nozzle diameter (mm)	Solid content (% w/w)	Nozzle gas flow (L/min)
SDD – A	1.2	5	15
SDD – B	1.2	15	15
SDD – C	1.2	15	5
SDD – D	0.4	15	5
SDD – E	0.4	5	15
SDD – F	0.4	5	5
SDD – G	0.4	15	15
SDD – H	0.8	10	10
SDD – I	1.2	5	5

Results

The spray drying process successfully converted the crystalline ETO to an amorphous form, confirmed by XRPD and DSC testing. All x-ray diffractograms had the typical “amorphous halo”, with no peaks indicative of crystalline ETO (Figure 1).

Figure 1. X-ray Diffractograms of Amorphous Solid Dispersions (ASD), Drug and Polymer

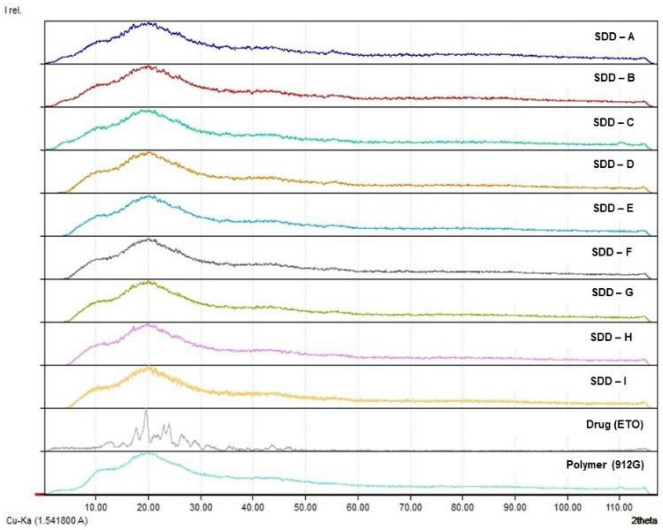

DSC results demonstrated the absence of a crystalline melting peak for all formulations when compared to the crystalline drug (Figure 2a and 2b). All ASD samples showed a single glass transition temperature (Tg) indicating that the amorphous API was homogenously dispersed into the polymer.

Figure 2a. DSC Thermograms of Drug (ETO) and Polymer (HPMCAS 912G)

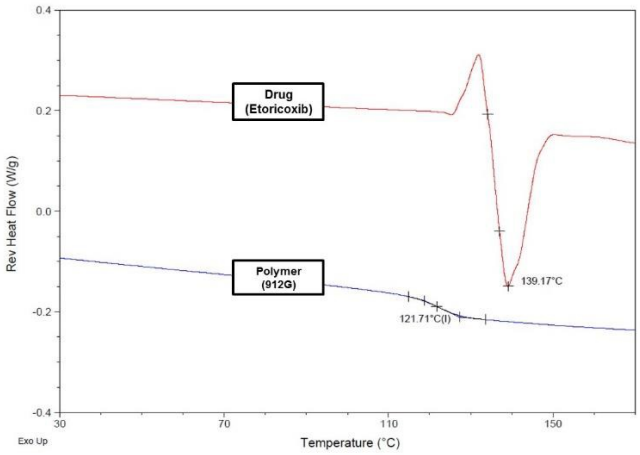

Figure 2b. DSC Thermograms of ETO:HPMCAS ASD

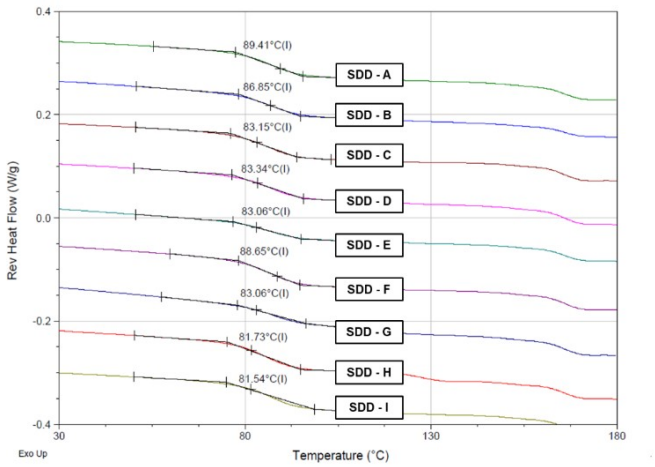

Although SEM images of the ASD particle surfaces did not show presence of detectable crystalline API, the SEM images (Figure 3) and particle size distribution results (Table 2) did show that adjustments to the process parameters impacted particle size and shape. Increases in nozzle diameter size to 1.2 mm and solids content to 15% w/w, resulted in an increased ASD particle size; which in turn reduced bulk density (Table 2). However, opposite effect was observed with changes in nozzle gas flow. At high nozzle gas flow, the particle size was reduced while improving the powder density. This subsequently improved powder density.

Figure 3. SEM images of ASD particles (900x Magnification)

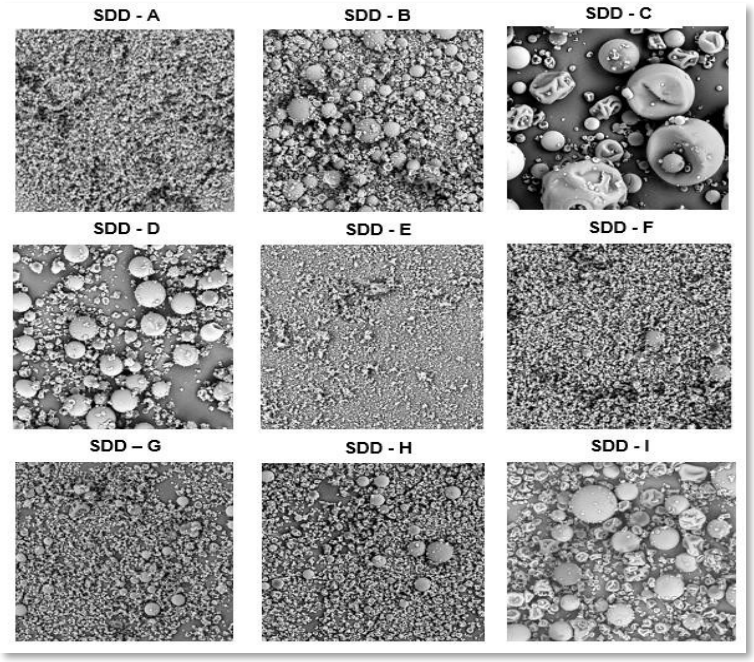

Loss on drying was performed to evaluate moisture or solvent content in the ASDs (Table 2). Larger particles were observed to have retained more moisture or solvent (SDD-C). Furthermore, the drug dissolution rate and apparent solubility of the larger particle formulations was low (Table 3). Smaller particle formulations had faster dissolution rates and high apparent solubility; this can be attributed to the increase in surface area of the particles.

Table 2. Powder Properties of ASDs

Batch Name ASD	True Density (g/mL)	Bulk Density (g/mL)	% LOD	d(0.1) µm	d(0.5) µm	d(0.9) µm
SDD – A	1.34	0.19	3.36	1.066	2.761	5.6
SDD – B	1.34	0.22	3.31	2.084	8.805	26.5
SDD – C	1.47	0.12	4.41	13.943	58.115	115.5
SDD – D	1.37	0.16	2.78	3.434	18.96	44.5
SDD – E	1.33	0.20	2.82	0.681	1.445	3.0
SDD – F	1.32	0.20	2.85	1.171	2.141	6.8
SDD – G	1.34	0.19	2.88	1.071	3.871	10.9
SDD – H	1.33	0.18	2.47	1.372	4.891	11.6
SDD – I	1.36	0.20	3.00	3.93	22.612	57.5

Table 3. Apparent Solubility and % Dissolution at 15 min for ETO and SDDs in Phosphate Buffer pH 6.8

Batch Name ASD	% Dissolution at 15 min	Apparent Solubility at 1 hour (µg/mL)
ETO Powder	11.31	50.32
SDD – A	90.89	93.18
SDD – B	86.52	92.07
SDD – C	71.82	84.09
SDD – D	78.91	90.02
SDD – E	89.73	92.63
SDD – F	89.27	90.76
SDD – G	84.98	92.33
SDD – H	95.50	96.59
SDD – I	84.85	88.92

In the majority of the ASD samples approx. 80% of the drug dissolved after 30 minutes (Figure 4). Overall, all ASDs demonstrated improved dissolution rates and apparent solubility of ETO compared to the crystalline drug (Table 3).

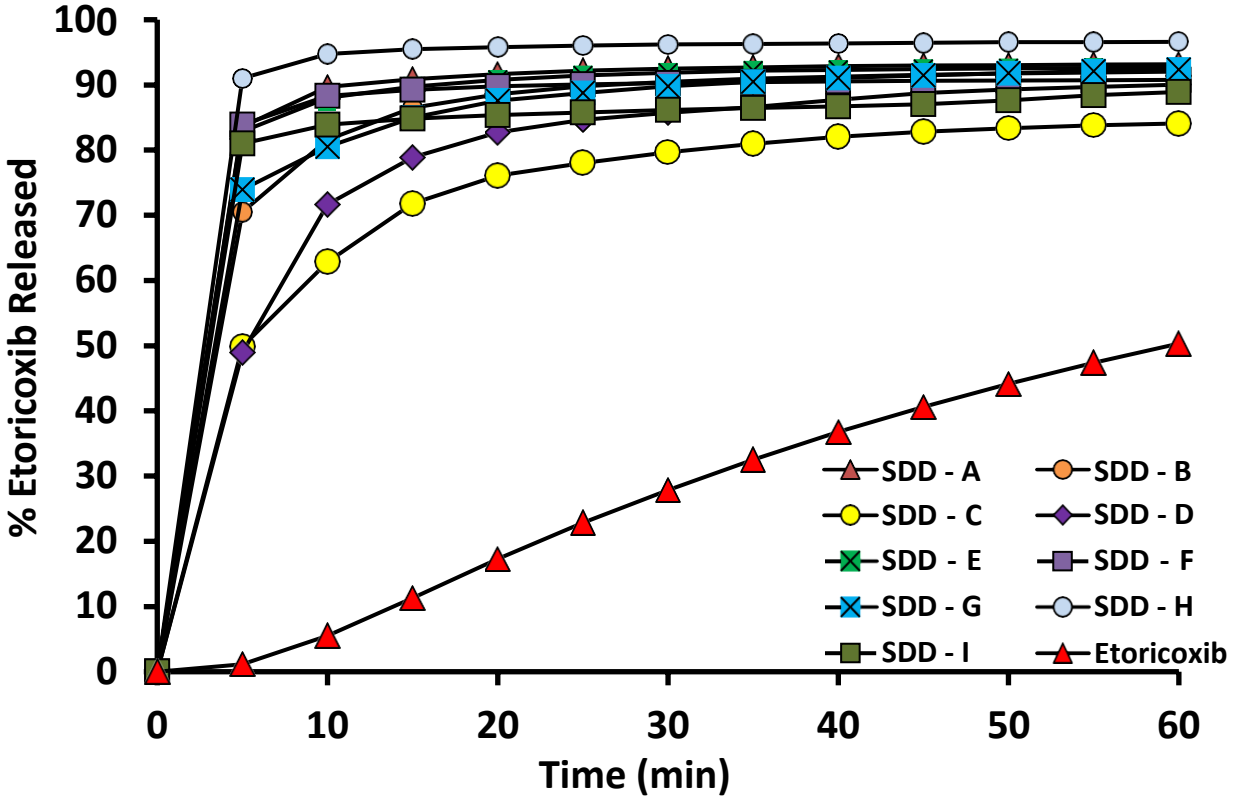

Figure 4. Dissolution of ASD (100 mg dose) vs. Etoricoxib

Figure 5. Effect of Process Parameters on (A) Mean Particle Size (d50) and (B) % Drug Release at 15 min.

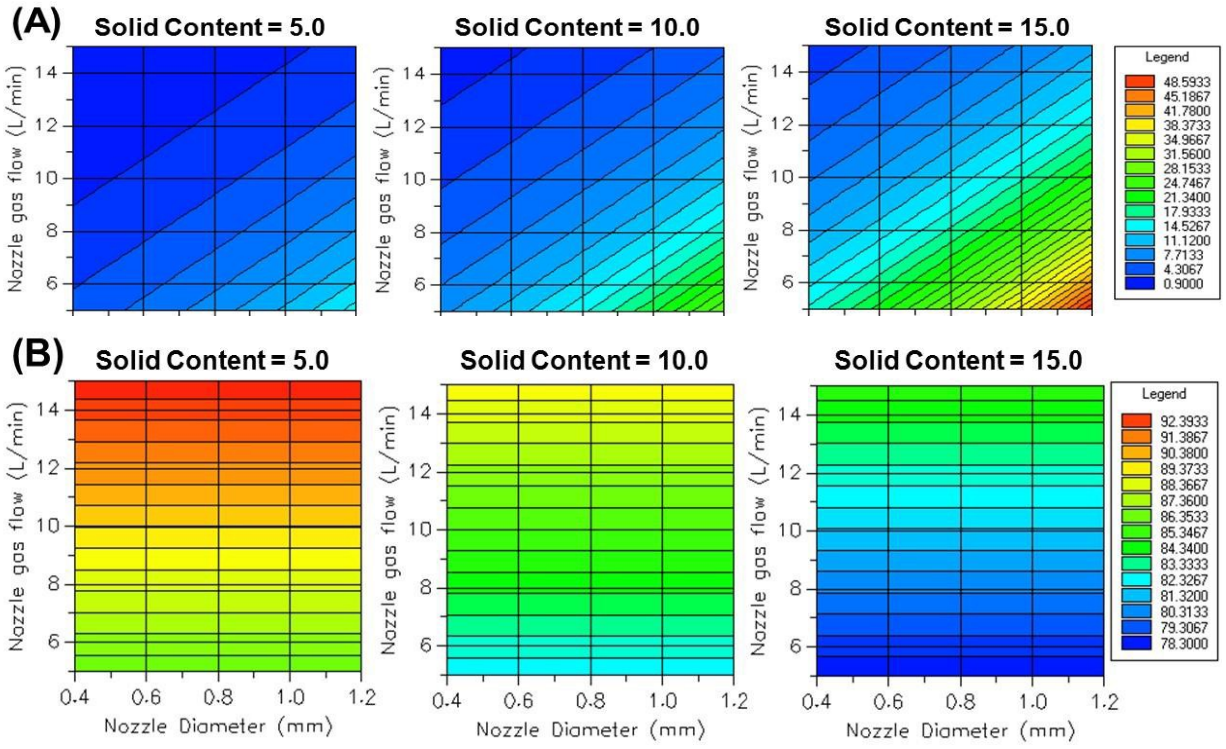

Using 2D contour plot analysis changes to process parameters that can impact ASD particle size and dissolution rate were confirmed. Contour plots, in Figure 5a and 5b, depict the effect of nozzle diameter and nozzle gas flow at different solids on mean particle size and drug release, respectively. The combination of high nozzle diameter, low gas flow and high solids produced larger particle sizes (>48.5 µm) (Figure 5a); this resulted in slower drug release: <78.3%) in 15 min (Figure 5b). Whereas, low nozzle diameter, high nozzle gas flow and low solids produced smaller particle sizes (<4 µm). This resulted in faster drug release: >92.4% at 15 min (Figure 5b).

Conclusions

Amorphous solid dispersions comprising ETO and AFFINISOL™ HPMCAS were successfully produced via spray drying. Variations of nozzle diameter, solids levels and nozzle gas flow impacted the powder properties and dissolution rate of the ASDs. The combination of nozzle diameter size and solids content influenced particle shape and size. Increasing nozzle gas flow also impacted particle sizes as well. This information can be greatly useful in the development of ASD tablet formulations. Adjustments to these conditions may assist in achieving desired powder properties while also increasing solubility and dissolution rate of a poorly soluble drug.

For more information, contact your Colorcon representative or call:

North America	Europe/Middle East/Africa	Latin America	India	China
+1-215-699-7733	**+44-(0)-1322-293000**	**+54-1-5556-7700**	**+91-832-6727373**	**+86-21-61982300**

You can also visit our website at **www.colorcon.com**